

Left atrial wall thickness of the pulmonary vein reconnection sites during atrial fibrillation redo procedures

Short title: atrial wall thickness at redo

Cheryl Teres MD; David Soto-Iglesias MSc, PhD; Diego Penela MD, PhD; Beatriz Jáuregui MD, MSc; Augusto Ordoñez MD; Alfredo Chauca MD; Marina Huguet MD, PhD; Carlos Ramírez MD, Guillermo Oller MD; Agustí Jornet MD, Jordi Palet MD, David Santana MD, Alejandro Panaro MD; Giuliana Maldonado MD; Gustavo de Leon MD; Belen Gualis MD; Gustavo Jimenez-Britez MD, PhD; Arturo Evangelista MD, PhD; Julio Carballo MD; José T. Ortiz-Perez MD, PhD, Antonio Berruezo MD, PhD

Heart Institute, Teknon Medical Center, Barcelona, Spain

FUNDING INFORMATION

Dr Teres was funded by the research fellowship grant of the Swiss Heart Rhythm Foundation.

CONFLICT OF INTEREST

Dr. Berruezo is stockholder of ADAS 3D Medical. Dr. Soto-Iglesias is an employee of Biosense Webster. The other authors have no other relevant affiliations or financial involvement with any organization or entity with a financial interest in or financial conflict with the subject matter or materials discussed in the manuscript apart from those disclosed.

DATA AVAILABILITY

Data might be available upon request

Corresponding author:

Antonio Berruezo,
Heart Institute, Teknon Medical Center,
C/ Vilana 12, 08022, Barcelona, Spain.
Email: antonio.berruezo@quironsalud.es

This article has been accepted for publication and undergone full peer review but has not been through the copyediting, typesetting, pagination and proofreading process, which may lead to differences between this version and the [Version of Record](#). Please cite this article as [doi: 10.1111/pace.14222](#).

This article is protected by copyright. All rights reserved.

Word count: 3991

STRUCTURED ABSTRACT

Background: Left atrial wall thickness (LAWT) has been related to pulmonary vein (PV) reconnections after atrial fibrillation (AF) ablation. The aim was to integrate 3D-LAWT maps in the navigation system and analyze the relationship with local reconnection sites during AF-redo procedures.

Methods: Consecutive patients referred for AF-redo ablation were included. Procedure was performed using a single catheter technique. LAWT maps obtained from multidetector computerized tomography (MDCT) were imported into the navigation system. LAWT of the circumferential PV line, the reconnected segment and the reconnected point, were analyzed.

Results: 60 patients [44 (73%) male, age 61 ± 10 years] were included. All reconnected veins were isolated using a single catheter technique with 55 minutes (IQR 47-67) procedure time and 75 seconds (IQR 50-120) fluoroscopy time. Mean LAWT of the circumferential PV line was 1.46 ± 0.22 mm. The reconnected segment was thicker than the rest of segments of the circumferential PV line (2.05 ± 0.86 vs 1.47 ± 0.76 , $p < 0.001$ for the LPVs; 1.55 ± 0.57 vs 1.27 ± 0.57 , $p < 0.001$ for the RPVs). Mean reconnection point wall thickness (WT) was at the 82nd percentile of the circumferential line in the LPVs and at the 82nd percentile in the RPVs.

Conclusion: A single catheter technique is feasible and efficient for AF-redo procedures. Integrating the 3D-LAWT map into the navigation system allows a direct periprocedural estimation of the WT at any point of the LA. Reconnection points were more frequently present in thicker segments of the PV line. The use of 3D-LAWT maps can facilitate reconnection point identification during AF-redo ablation.

KEYWORDS

Atrial fibrillation, atrial wall thickness, catheter ablation, gap identification.

ABBREVIATIONS LIST

AT atrial tachycardia

LAWT left atrial wall thickness

LPV left pulmonary vein

MDCT multidetector computerized tomography

PV pulmonary vein

PVI pulmonary vein isolation

RPV right pulmonary vein

WT wall thickness

INTRODUCTION

Circumferential pulmonary vein isolation (PVI) has become a mainstay in the treatment of AF, particularly in symptomatic patients with paroxysmal AF intolerant or refractory to medical treatment. (1) Despite the significant technical improvements occurred in the last decade, including contact force sensing catheters and the use of ablation indexes, creation of durable transmural lesions in the left atrium remains a main challenge of PVI procedures. Post-ablation pulmonary vein reconnections are responsible for atrial fibrillation/tachycardia (AT) recurrences owing to incomplete non-transmural ablation lesions that translate into gaps on ablation lines at different time lapses.²⁻⁴

The left atrial wall is a thin structure with heterogeneous thickness, ranging from < 1 mm to > 5 mm, with an important inter and intra-patient variability. This variability in LAWТ is the result of a complex array of three-dimensional muscular strands.⁵ Isolation of pulmonary veins can be limited by inability to create transmural lesions in areas with higher LAWТ.⁶ In

consequence, LAWT was described as an independent predictor of AF recurrence and it might even be a predictor of transition from paroxysmal to chronic AF.⁷

The aim of the present study was to analyze the relationship between reconnection gaps and local LAWT by integration of LAWT maps into the navigation system during AF-redo procedures, as well as to evaluate the feasibility of a single catheter approach in this setting.

METHODS

Patient Sample

Consecutive patients referred for AF-redo ablation between November 2018 and December 2019 at a single center were included. It was accepted that first ablation procedures could have been performed at any center and with any technique. In all patients a multi-detector cardiac tomography (MDCT) study was performed prior to the re-ablation procedure. MDCT-derived maps with LAWT information were then imported into the navigation system for aiding the procedure. The minority of patients in whom all the PVs were isolated at the AF-redo procedure were excluded from the analysis, since comparison of LAWT in these cases was deemed not interpretable. No patient was excluded because of poor image quality. The study complied with the Declaration of Helsinki. The local Ethics Committee approved the study protocol and all included participants provided written informed consent before the procedure.

Pre-procedural multi-detector cardiac tomography (MDCT) and image processing

MDCT was performed with a dual source SOMATOM™ Definition Flash 128 slice, scanner (Siemens Healthineers, Erlangen, Germany) or a Revolution™ scanner (General Electric Healthcare). Images were acquired during an inspiratory breath-hold using retrospective ECG-gating technique with tube

current modulation set between 50% and 100 % of the cardiac cycle. Angiographic images were acquired during the injection of a 100 mL bolus of Iopromide 370 mg I/mL (Ultravist, Bayer Hispania, Barcelona, Spain) at a rate of 3mL/s. The administered radiation dose with this method is 160 mGy × cm which accounts for 3 mSv and approximately 27mGy total dose. Data was transmitted to the workstation for post-processing and reconstructed into axial images with slice thickness of 0.625 mm.

Image post-processing

MDCT images were analyzed with ADAS 3D™ software (ADAS3D Medical, Barcelona, Spain) to obtain a 3D LAWT map by applying a 3-step algorithm: i) the endocardial layer was delineated by means of a semi-automatic segmentation based on pixel intensity thresholds; ii) the epicardial layer was defined manually with a multi-slice approach on the long-axis projection, with a mean of 20±7 epicardial delineations per patient; iii) Finally, wall thickness (WT) was automatically computed at each point as the distance between each endocardial point and its projection to the epicardial shell (Figure 1). These three steps result in a 3D WT map that can be imported into CARTO navigation system (Biosense Webster, Diamond Bar, California, US) by using the Carto Merge tool. A color code was used to create a range of thicknesses (red < 1 mm, yellow 1-2 mm, green 2-3 mm, blue 3-4 mm and purple > 4 mm). Intra and inter observer variability of the proposed method were evaluated. For this purpose, 3 independent observers with different levels of experience performed twice the WT segmentation in a random sample of 10 cases.

Ablation procedures

The majority of the first procedures were performed by the same operator, under conscious sedation, with a single catheter, contact force-guided dragging technique and an energy between 30-40 W. Esophageal temperature was not monitored. Energy setting, application duration, and contact force of the first procedure were not available for analysis.

Redo interventions were performed on uninterrupted oral anticoagulation and under general anesthesia with a single catheter technique using an 8F Mullins non-steerable transseptal introducer sheath (Medtronic, Minneapolis, MN, USA) and a 3.5 mm irrigated tip catheter (NaviStar[®] ThermoCool[®], Biosense Webster, Diamond Bar, CA, USA). Hemodynamic monitoring was done with a radial arterial catheter. Peri-procedural anticoagulation was performed with a first 1 mg/kg IV dose of unfractionated heparin immediately before transseptal puncture and periodic activated clotting time sampling was obtained every 30 minutes to guide further bolus dosing with a target between 300 and 350 seconds. Transseptal puncture was obtained with transesophageal echocardiogram guidance. After that, a fast-anatomical map (FAM) of the entire left atrial anatomy and the pulmonary veins was acquired with the ablation catheter to integrate it with the LAWT map within the spatial reference coordinates of the CARTO system.

Reconnection site identification

Analysis of the pulmonary vein reconnections was done in sinus rhythm. For patients with persistent AF, cardioversion was either scheduled days before the procedure or performed at the procedure once the patient was under general anesthesia. PV reconnection sites were identified by analyzing electrograms on the EP recording system (EP-TRACER, Schwarzer Cardiotek, Heilbronn, Germany), or

on the CARTO navigation system, recorded with the ablation catheter according to a systematic, standardized local approach. A PV reconnection was defined as the presence of a PV potential, either a high amplitude sharp electrogram (EGM) inside the vein or a low amplitude fragmented EGM near the circumferential PV line that was identified with the ablation catheter inside the vein and/or if capture of atrial rhythm was achieved after programmed PV stimulation in any point inside the circumferential PV line.^{8,9} The reconnection site was defined as the point with the earliest PV electrogram (PV-EGM) along the circumferential PV line. For this purpose, the EP recording was synchronized in a beat-to-beat manner, during stable sinus rhythm and a fixed PR interval, with a caliper in the peak of the QRS in the surface ECG marked as reference. The ablation catheter was sequentially placed on each segment of the circumferential PV line and the earliest PV potential with respect to the reference caliper is considered the reconnection site (Figure 2). If electrical activation inside the vein was still observed after ablation of the first designated reconnection point, and the local fusion between the atrial electrogram and the PV electrogram was observed at different distant points, multiple reconnection points were determined the process was repeated until all the reconnected points were identified (Figure 3). Each one of these points was considered as a reconnection and included in the analysis. RF was applied at the reconnection sites until complete isolation of all PVs was achieved. Ablation parameters were 35-50W, 45°C., with ablation time adapted to the WT with a standard pre-defined local protocol (Table 2). The procedural endpoint was PV disconnection, which was confirmed by entry block with absence of PV potentials inside the vein with the ablation catheter placed sequentially in each segment inside the circumferential PV line, and exit block by proving absence of conduction when pacing (11 mA, 2ms) from inside the circumferential PV line sequentially at each segment.

Wall thickness definitions and reconnection site analysis

In the first ten cases, the operator was blinded to the LAWT, since it was analyzed retrospectively. For the remaining cases the LAWT information was available during the procedure. After the procedure, LAWT maps were exported from CARTO for analysis into a Matlab customized software. The circumferential PV lines were divided following the 16-segment model (Figure 4). WT was calculated for the whole circumferential PV line and for each segment individually. During the ablation procedure, tags were generated on the 3D LAWT map for each identified reconnection site, using standard CARTO tags. The LAWT under the tag was considered the reconnection point WT. The segment where the point was located was considered a reconnected segment. Both, the reconnected point WT and the reconnected segment WT values were analyzed for each identified reconnection site. These values were compared with the WT of the non-reconnected segments of the circumferential PV line.

Follow-up

Patients were scheduled to be followed-up at the outpatient clinic at 1, 3, 6 and 12 months. Each evaluation included an ECG and a 24-hour Holter monitoring. Recurrence was defined as any documented AF/AT episode lasting more than 30 seconds during this period or symptoms suggesting recurrence.

Statistical Analysis

All applicable statistical tests are 2-sided and performed using a 5% significance level. Continuous variables are presented as mean \pm standard deviation or median (range or interquartile range if data

are skewed) if not normally distributed. To compare means of two variables the Student's t test, Mann-Whitney U test, or Anova test were used, as appropriate. Categorical variables were expressed as total number (percentages) and compared between groups using Chi-square or Fisher's exact test. Statistical analysis was performed using IBM SPSS Statistics for Macintosh, version 25.0 (IBM Corp. Released 2017; Armonk, NY: IBM Corp.) and customized code for the Matlab statistics toolbox (Matlab R2010a, The Mathworks, Inc., Natick, MA, USA).

RESULTS

Patient population

Baseline characteristics are summarized in Table 1. Sixty patients were included. Mean age 61 ± 10 years, 43 (72%) male. Median time since first ablation was 19,5 months (IQR 9-55). Mean number of previous ablations was $1,1\pm 0,4$. Total number of previous ablations was 1 in 54 (90%) patients; 2 in 5 (8,3%) patients and 3 in 1 (1,7%) patient. All previous ablations were performed with RF ablation except for one case done with cryoablation. At first ablation, 38 out of 60 (63%) of patients presented with paroxysmal AF and 22 out of 60 (37%) with persistent AF. Three patients were excluded since all PVs were isolated at the AF-redo procedure. No patient was excluded because of impossibility to perform MDCT owing to severe kidney failure.

Acute procedural characteristics

Median procedure time was 55 minutes (IQR 47-67). Merge time (FAM acquisition + MDCT merging on CARTO) was 12 minutes (IQR 10-15). Median fluoroscopy time was 1.25 min (IQR 0.8-2) with a Fluoroscopy dose of $1,5 \text{ mGy/m}^2$ (IQR 0,8-3,2).

There was a total of 113 PV reconnections, accounting for a mean of 1.89 ± 0.37 reconnected veins per patient. After analyzing the circumferential PV line, a total of 316 reconnection sites were identified with a mean of 4 ± 2 per patient. By applying radiofrequency (RF) in the identified reconnection sites, all PVs were disconnected. Median RF time was 5,8 min (IQR 2,5-8,2); 2,9 min (IQR 0,5-3,8) for the right PVs and 1,9 min (IQR 1,6-4,95) for the left PVs. There was 1 procedure related complication that consisted in an arterial pseudoaneurysm that did not require surgical treatment.

Atrial wall thickness measurements and reconnection sites

Mean LAWT of the circumferential PV line was 1.46 ± 0.22 mm. The circumferential PV line was thicker in the LPVs as compared to the RPVs (1.56 ± 0.51 vs. 1.30 ± 0.37 mm $p=0.004$ respectively). In the LPVs the antero-inferior, anterior carina and antero-superior segments were the thicker; and the posterior-carina was the thinnest. In the right PVs the thicker segments were the antero-superior, anterior-carina and the roof; and the thinnest was the inferior segment. Figure 5 shows the mean LAWT of each segment.

The reproducibility assessment showed an intra and inter observer reproducibility of the endocardial layer (automatic segmentation) for points closer than 1mm of $99 \pm 0.9\%$ and $95 \pm 5\%$, respectively. Intra and interobserver reproducibility of the epicardial layer (manual segmentation) for points closer than 1mm was $82 \pm 10\%$ and $78 \pm 7\%$, respectively. This traduced on an overall mean intra-observer distance between discordant points of 0.1 mm on the endocardium and 0.3 mm on the epicardium and an inter-observer mean distance of 0.2 mm on the endocardium and 0.6 mm on the epicardium.

In total, 113 PV reconnections were identified. 56 out of 60 (93%) patients presented reconnections in the RPVs and 57 out of 60 (95%) in the LPVs, $p=0.58$. None of the 16 segments was spared from reconnections.

The most frequent location for reconnections at both sides was the anterior carina, which was reconnected on 65% of cases on the LPVs (mean WT 2.05 ± 0.86 mm) and 52% of cases on the RPVs (mean WT of 1.55 ± 0.57 mm). As compared with the rest of segments of the circumferential PV line, the reconnected segment WT was higher (2.05 ± 0.86 vs 1.47 ± 0.76 , $p < 0.001$ for the LVPs; 1.55 ± 0.57 vs 1.27 ± 0.57 , $p < 0.001$ for the RPVs). The reconnected point WT was also thicker as compared with the rest of the circumferential PV line [total 1.72 ± 0.86 vs 1.46 ± 0.22 , $p = 0.02$; LVPs 1.98 ± 1.07 vs 1.49 ± 0.76 $p = 0.004$; RPVs 1.49 ± 0.58 vs 1.27 ± 0.57 $p = 0.03$ s], as Figure 6 shows. Mean reconnection point WT was at the 82nd percentile of the circumferential PV line WT in the LPVs and at the 82nd percentile in the RPVs. Figure 5 shows the percentage of reconnection at each segment in the 16-segment model.

Follow-up

Twelve out of sixty (20%) patients presented a recurrence during a mean follow-up of 7 ± 3 months (Supplementary Table S1). Recurrence was more frequent in patients with persistent AF than in patients with paroxysmal AF (41% vs 8% recurrence rate respectively, $p < 0.01$). Patients presenting a recurrence had a larger LA diameter (44 ± 4 mm vs 40 ± 6 mm, $p < 0.01$), lower LVEF (55 ± 10 vs 59 ± 3 , $p = 0.01$) and presented an underlying cardiomyopathy more frequently (2 hypertrophic, 1 ischemic, 3 hypertensive) [8 out of 48 (16%) patients in the non-recurrence group vs 6 out of 12 (50%) in the recurrence group, $p = 0.05$].

DISCUSSION

The present study is the first one reporting the feasibility of integrating the 3D LAWT maps into the navigation system, allowing for a direct intraprocedural estimation of the WT at any point of the LA and therefore at the reconnected points. The study shows that the mean LAWT at the identified reconnected points was thicker than the rest of the circumferential PV line. The study also proves the feasibility and usefulness of a simplified method for performing the AF-redo procedure using a single catheter technique that improves efficiency by obtaining short procedure and fluoroscopy times as compared with the literature standards.^{11,12} The use of 3D LAWT maps can facilitate reconnection point identification during AF-redo ablation by permitting to focus mapping in the thicker points and segments.

Single Catheter Approach

The single catheter approach has already been described for PV isolation at first ablation procedures,^{9,10} showing that this method is cost-saving, and non-inferior regarding AF recurrences in the mid-term. The present study reports on a single catheter approach for performing AF-redo procedures in which the ablation line must be mapped in each and every case, with the implementation of a simplified approach for identifying the electrical breakthrough based on timing of the local PV electrogram without need of a further catheter for reference⁸ (Figure 2). This as opposed to first ablations where the high rate of first pass isolation allows for avoidance of this step. The method is feasible, as all reconnected veins could be isolated by applying RF in the reconnection sites identified with this approach. The procedure workflow simplification results in high efficiency with a median procedure time under one hour and a very low fluoroscopy time and dose. Moreover, this approach had a very low complication rate (1.5%) probably related to the use of a single catheter and a single vascular and transeptal access.

MDCT 3D LAWT maps

Imaging techniques have led to better understanding of PV anatomy and more efficient procedure planning.¹³ Even though many limitations have been described on MDCT atrial wall thickness measurement for previous generations of scanners, modern machines allow for sub-millimetric resolution. In fact, CT atrial wall thickness measurements have been reliably validated on a porcine model¹⁴, and 3D LAWT maps have already been generated from contrast cardiac computed tomography images.¹⁵ Having in mind that the spatial resolution of the MDCT is 0.4 mm, we assume that the variability of the proposed method is low and the expected clinical repercussion of this variability, is also presumably low. Although further evidence is needed to confirm this low clinical impact of the variability. Of all the determinants of lesion creation, LAWT is one key element that has been evaluated in some retrospective analysis but has never been integrated on the navigation system during the procedure. Importing the LAWT map derived from the MDCT into the navigation system allows for real-time knowledge of the atrial WT in contact with the catheter tip. This feature might be useful in different settings, as for instance in adapting energy delivery to avoid excessive application in thinned wall segments improving safety or delivering more energy in thicker regions in order to obtain more durable lesions¹⁶; allowing to focus mapping at the thicker points looking for reconnections in the ablation line during AF-redo procedures; and personalizing sites of RF application when drawing ablation lines to avoid thicker segments. Thus, this new imaging tool, opens the door for future diagnostic and therapeutic strategies using the integration of 3D LAWT maps into the navigation system.

LAWT and gap identification

The result of this pilot study confirms previous observations from retrospective studies, on that atrial WT is a major determinant of lesion transmuralty and that PV reconnections occur more frequently in thicker parts of the PV circumferential line. We have found that the more frequently reconnected sites are those with thicker atrial WT, in particular the right and left anterior carinas. In fact, previous histological¹⁷ and imaging¹⁸ studies have shown that the left atrial ridge is the thickest structure around the circumferential PV lines and that is also where reconnection sites were more frequently found in this study. Nevertheless, despite an excellent spatial resolution which is the main robustness of CT scan, the contrast resolution of this technique is lower than that of MRI, because the difference in x-ray attenuation between different tissues is modest. In consequence, CT image cannot distinguish myocardium from other tissues especially at the very thin LA wall and therefore, it is important to bear in mind that a thick LA wall does not necessarily mean a thick myocardial sleeve.

Follow-up

A 20% recurrence rate after de AF-redo ablation was observed during follow-up, this is in line with previous observations.¹⁰ Recurrences were more frequent in patients presenting known predictors of recurrence after a first ablation as larger atrial diameter¹⁹; presence of a previous structural heart disease²⁰; and persistent AF at first ablation procedure.²¹ The recurrence rate in patients with paroxysmal AF was as low as 8%, validating the long-term efficacy of a single catheter ablation technique for AF-redo procedures.

Clinical implications

This study describes the clinical usefulness of MDCT derived 3D LAWT maps to allow better identification of thicker atrial wall regions which is where reconnections are more frequently located. Our results not only stress the importance of atrial WT as a determinant of long-term lesion transmuralty but also set the stage for a wide use of 3D LAWT maps at first AF ablation procedures to probably increase efficacy and safety given the fact that adapting the ablation parameters to the local WT is a long-time unmet need in the AF ablation field. Besides, the use of 3D LAWT maps could allow for a shortening of the procedure time and RF delivery and fluoroscopy time since gap identification can in many cases be aided by the map. However, further prospective studies are needed to validate this hypothesis.

Furthermore, we adopted the single catheter approach for determining and ablating the reconnection site. The combination of these methods results in a very efficient and less invasive procedure with very good acute and mid-term outcomes. Once again, prospective studies are needed to compare the safety and efficacy of this approach with regard the conventional multicatheter approach.

Limitations

The main limitation of this study is the lack of a control group for comparison. Besides, procedure characteristics of the first ablation were not available for analysis. Hence, an association between the lack of stability, the applied power settings or the presence of gaps on the circumferential PV line and the distribution of reconnection sites cannot be excluded, especially in some segments where it is difficult to ensure good catheter stability during RF application, as the left anterior carina.

Furthermore, it is possible that RF application at first ablation itself might directly affect LA wall thickness through scar involution and consecutive tissue remodeling. Another limitation is that the LAWT method depends on contrast enhanced MDCT acquisition, which is contraindicated in patients with severe kidney failure, needs special preparation in patients with contrast medium allergy and implies radiation exposure. Nevertheless, fluoroscopic requirements for the presented method are lower to what has been reported on multicenter international registries²² and what has been found on recent prospective trials²³. Therefore, even though the need for a MDCT might imply additional radiation exposure, the overall radiation dose administered is still reasonable. That said, evidence is lacking, and our results warrant further research. Finally, multielectrode catheters were not used to identify the reconnection sites. However, all pulmonary veins were successfully isolated, and the mid-term recurrence rate was low using a single 4-electrodes catheter. Finally, we modulated RF delivery at the redo procedure based on empiric parameters. Further studies are needed to evaluate the optimal parameters of RF application according to the LAWT.

CONCLUSION

3D LAWT maps can be obtained from MDCT scan and be integrated into the navigation system. It allows for a direct periprocedural estimation of the WT at any point of the LA. Reconnection points are more frequently present in the thicker segments of the circumferential PV line and usually are the thickest point of the segment. A single catheter approach is feasible, efficient and safe during AF-redo procedures, allowing to easily identify the reconnected segment with a low recurrence rate at mid-term.

REFERENCES

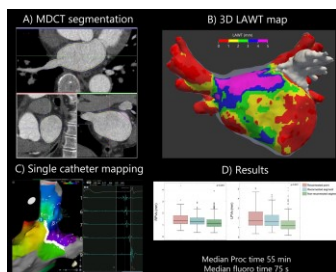
1. Calkins H, Hindricks G, Cappato R, Kim YH, Saad EB, Aguinaga L, Akar JG, et al. 2017 HRS / EHRA / ECAS / APHRS / SOLAECE expert consensus statement on catheter and surgical ablation of atrial fibrillation. *Europace* 2018;20(1):e1-e160. doi:10.1093/europace/eux274.
2. Ouyang F, Tilz R, Chun J, Schmidt B, Wissner E, Zerm T, Neven K, et al. Long-Term Results of Catheter Ablation in Paroxysmal Atrial Fibrillation From a 5-Year Follow-Up. *Circulation* 2010;122:2368–77. doi: 10.1161/CIRCULATIONAHA.110.946806.
3. Cappato R, Negroni S, Pecora D, Bentivegna S, Lupo PP, Carolei A, Esposito C et al. Prospective assessment of late conduction recurrence across radiofrequency lesions producing electrical disconnection at the pulmonary vein ostium in patients with atrial fibrillation. *Circulation* 2003;108(13):1599–604. doi: 10.1161/01.CIR.0000091081.19465.F1.
4. Kuck K-H, Hoffmann BA, Ernst S, Wegscheider K, Treszl A, Metzner A, Eckardt L, et al. ; Gap-AF–AFNET 1 Investigators. Impact of complete versus incomplete circumferential lines around the pulmonary veins during catheter ablation of paroxysmal atrial fibrillation: results from the Gap-Atrial Fibrillation-German Atrial Fibrillation Competence Network 1 Trial. *Circ Arrhythm Electrophysiol*. 2016 Jan;9(1):e003337. doi: 10.1161/CIRCEP.115.003337
5. Ho SY, Sanchez-Quintana D. The importance of atrial structure and fibers. *Clin Anat* 2009;22(1):52–63. doi: 10.1002/ca.20634.
6. Kistler PM, Ho SY, Rajappan K, Morper M, Harris S, Abrams D, Sporton SC, et al. Electrophysiologic and anatomic characterization of sites resistant to electrical isolation during circumferential pulmonary vein ablation for atrial fibrillation: a prospective study. *J Cardiovasc Electrophysiol* 2007;18(12):1282–8. doi: 10.1111/j.1540-8167.2007.00981.x.
7. Nakamura K, Funabashi N, Uehara M, Ueda M, Murayama T, Takaoka H, Komuro I, et al. Left

- atrial wall thickness in paroxysmal atrial fibrillation by multislice-CT is initial marker of structural remodeling and predictor of transition from paroxysmal to chronic form. *Int J Cardiol* 2011;148(2):139–47. doi: 10.1016/j.ijcard.2009.10.032.
8. Arenal A, Atea L, Datino T, González-Torrecilla E, Atienza F, Almendral J, Sánchez A, et al. Identification of conduction gaps in the ablation line during left atrium circumferential ablation: facilitation of pulmonary vein disconnection after endpoint modification according to electrogram characteristics. *Heart Rhythm* 2008;5(7):994–1002. doi: 10.1016/j.hrthm.2008.03.061.
 9. Pambrun T, Combes S, Sousa P, Bloa ML, El Bouazzaoui R, Grand-Larrieu D, Thompson N, et al. Contact-force guided single-catheter approach for pulmonary vein isolation: Feasibility, outcomes, and cost-effectiveness. *Heart Rhythm* 2017;14(3):331-338. doi: 10.1016/j.hrthm.2016.12.008.
 10. Dong J, Liu X, Long D, Yu R, Tang R, Lü F, Ma C. Single-catheter technique for pulmonary vein antrum isolation: is it sufficient to identify and close the residual gaps without a circular mapping catheter? *J Cardiovasc Electrophysiol*. 2009 Mar;20(3):273-9.
 11. Zeljkovic I, Knecht S, Spies F, Reichlin T, Osswald S, Kühne M, Sticherling C. Paroxysmal atrial fibrillation recurrence after redo procedure-ablation modality impact. *J Interv Card Electrophysiol* 2020;57(1):77-85. doi: 10.1007/s10840-019-00694-w.
 12. Johner N, Shah DC, Giannakopoulos G, Girardet A, Namdar M. Evolution of post-pulmonary vein isolation atrial fibrillation inducibility at redo ablation: Electrophysiological evidence of extra-pulmonary vein substrate progression. *Heart Rhythm* 2019;16(8):1160–6. doi: 10.1016/j.hrthm.2019.02.026.
 13. Dong J, Calkins H, Solomon SB, Lai S, Dalal D, Lardo AC, Brem E, et al. Integrated

- electroanatomic mapping with three-dimensional computed tomographic images for real-time guided ablations. *Circulation* 2006;113(2):186–94. doi: 10.1161/CIRCULATIONAHA.105.565200.
14. Sun JY, Yun CH, Mok GSP, Liu YH, Hung CL, Wu TH, Alaiti MA, et al. Left Atrium Wall-mapping Application for Wall Thickness Visualisation. *Sci Rep.* 2018;8(1):4169. doi: 10.1038/s41598-018-22089-z.
 15. Bishop M, Rajani R, Plank G, Gaddum N, Carr-White G, Wright M, O'Neill M, et al. Three-dimensional atrial wall thickness maps to inform catheter ablation procedures for atrial fibrillation. *Europace* 2016;18(3):376-383. doi: 10.1093/europace/euv073.
 16. Soor N, Morgan R, Varela M, Aslanidi O V. Towards patient-specific modelling of lesion formation during radiofrequency catheter ablation for atrial fibrillation. *Eng Med Biol Soc* 2016;2016:489–92. doi: 10.1109/EMBC.2016.7590746.
 17. Cabrera JA, Ho SY, Climent V, Sanchez-Quintana D. The architecture of the left lateral atrial wall: a particular anatomic region with implications for ablation of atrial fibrillation. *Eur Heart J.* 2008;29(3):356–62. doi: 10.1093/eurheartj/ehm606.
 18. Mansour M, Refaat M, Heist EK, Mela T, Cury R, Holmvang G, Ruskin JN. Three-dimensional anatomy of the left atrium by magnetic resonance angiography: implications for catheter ablation for atrial fibrillation. *J Cardiovasc Electrophysiol.* 2006;17(7):719–23. doi: 10.1111/j.1540-8167.2006.00491.x.
 19. Berruezo A, Tamborero D, Mont L, Benito B, Tolosana JM, Sitges M, Vidal B, et al. Pre-procedural predictors of atrial fibrillation recurrence after circumferential pulmonary vein ablation. *Eur Heart J.* 2007;28(7):836–41. doi: 10.1093/eurheartj/ehm027.
 20. Lee SH, Tai CT, Hsieh MH, Tsai CF, Lin YK, Tsao HM, Yu WC, et al. Predictors of early and late

- recurrence of atrial fibrillation after catheter ablation of paroxysmal atrial fibrillation. *J Interv Card Electrophysiol.* 2004;10(3):221– 226. doi: 10.1023/B:JICE.0000026915.02503.92.
21. Themistoclakis S, Schweikert RA, Saliba WI, Bonso A, Rossillo A, Bader G, Wazni O, et al. Clinical predictors and relationship between early and late atrial tachyarrhythmias after pulmonary vein antrum isolation. *Heart Rhythm* 2008;5(5):679–85. doi: 10.1016/j.hrthm.2008.01.031
 22. Sciahbasi A, Ferrante G, Fischetti D, Miklin DJ, Sarandrea A, Schirripa V, Guarracini F, et al. Radiation dose among different cardiac and vascular invasive procedures: The RODEO study. *Int J Cardiol.* 2017 Aug 1; 240:92-96. doi: 10.1016/j.ijcard.2017.03.031.
 23. Quinto L, Cozzari J, Benito E, Alarcón F, Bisbal F, Trotta O, Caixal G, et al. Magnetic resonance-guided re-ablation for atrial fibrillation is associated with a lower recurrence rate: a case-control study. *Europace.* 2020 Dec 23;22(12):1805-1811. doi: 10.1093/europace/euaa252.

FIGURE LEGENDS



Central figure. A) Endocardial and epicardial layers delineation on MDCT. **B)** 3D LAWT map categorized for thickness ranges (color code: red < 1 mm, yellow 1-2 mm, green 2-3 mm, blue 3-4 mm and purple > 4 mm). **C)** Single catheter technique for identification of the reconnection site. **D)** Comparison of LAWT measurements on both pairs of veins.

LAWT: left atrial wall thickness; MDCT: multidetector computerized tomography

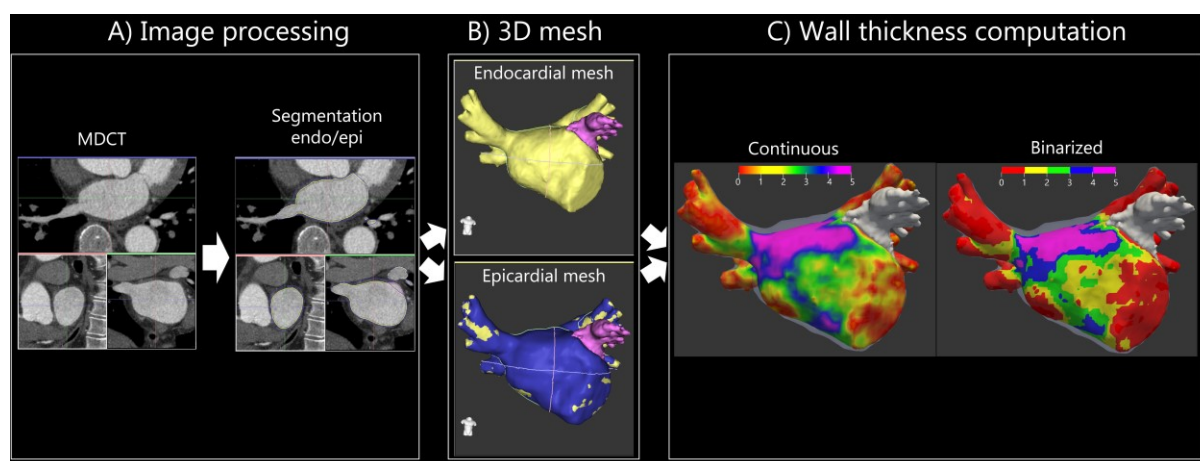


Figure 1. Segmentation pipeline of the 3D left atrial Wall thickness map. (A) Endocardial and epicardial layer delineation. **(B)** Endocardial and epicardial shells after semi-automatic segmentation in the endocardium and manual segmentation with a multi-slice approach in the epicardium. **(C)** Automatically computation of wall thickness as the distance between each endocardial point and its projection to the epicardial shell (color code: red < 1 mm, yellow 1-2 mm, green 2-3 mm, blue 3-4 mm and purple > 4 mm).

MDCT: multidetector computerized tomography

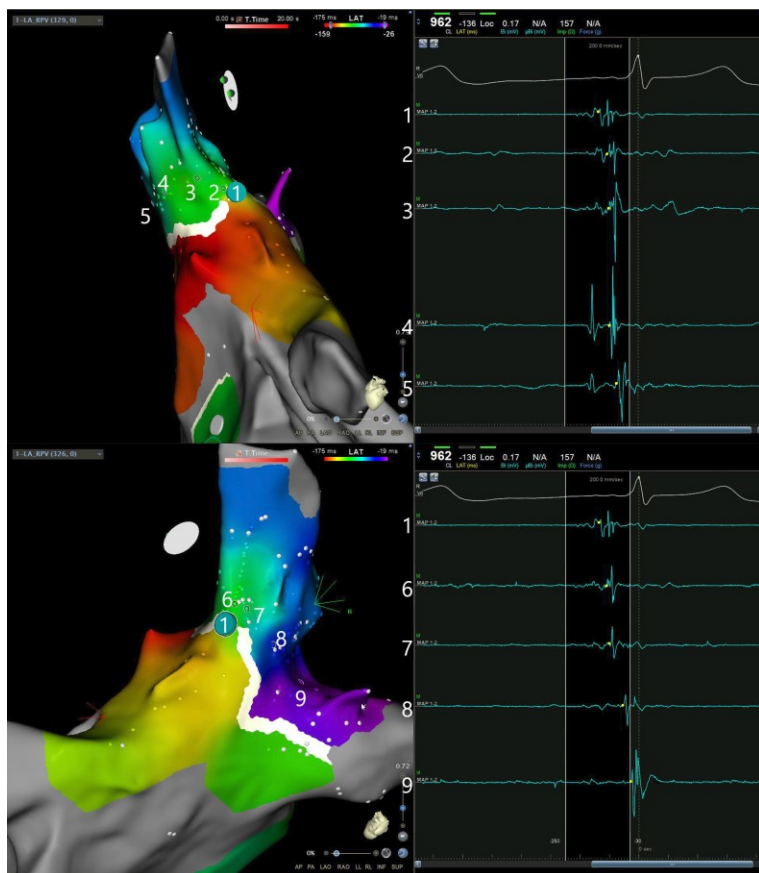


Figure 2. Reconnection site identification with a single catheter technique. PV reconnection sites were identified as the point with the earliest PV electrogram (PV-EGM) along the circumferential PV line. **TOP** antero-superior view of the left atrium with activation map of the right superior PV. Points 1-5 represent sites where local activation was annotated and the respective local electrogram is depicted on the right-hand side. **BOTTOM** Postero-superior view of the same case.

Accepted Article

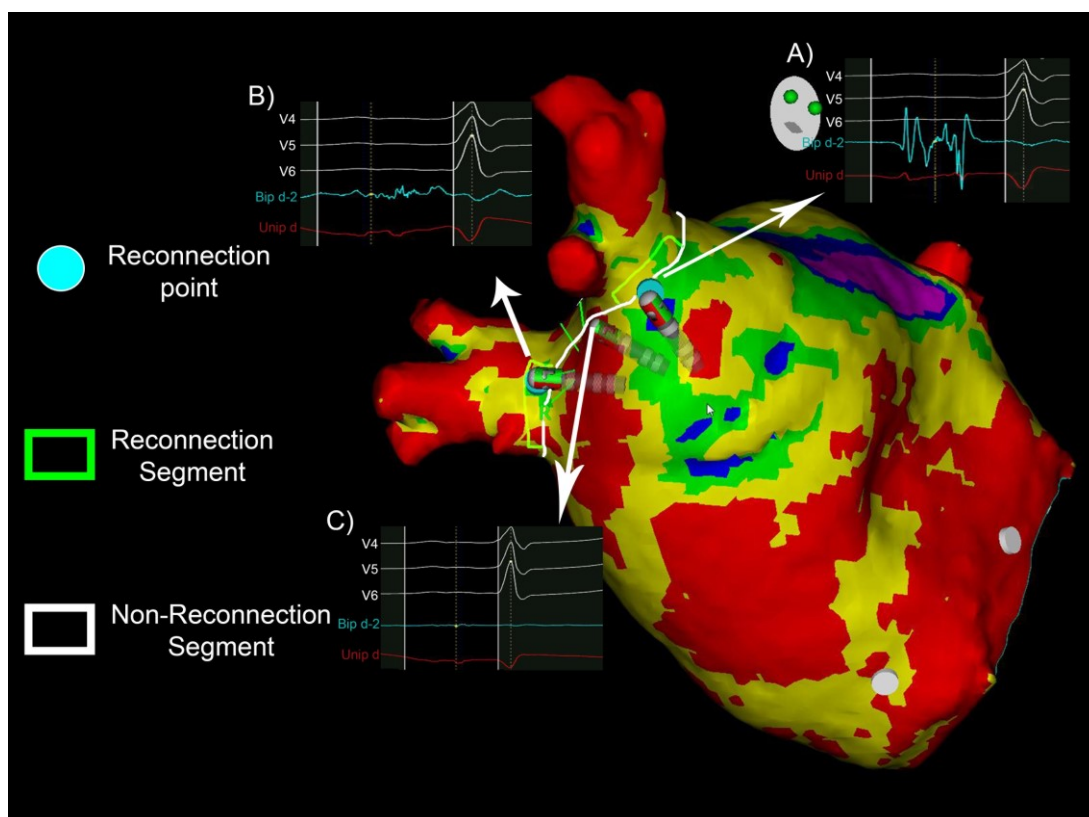


Figure 3. Example of a case with two pulmonary vein reconnections in the same vein pair. Low amplitude fragmented electrogram near the circumferential PV line on the antero-superior (A) and antero-inferior (B) segments of the right PVs. These reconnections were subsequently proved by capture of an atrial rhythm after pacing from the presumed reconnection site. The electrogram at the anterior carina (C) shows absence of local signal.

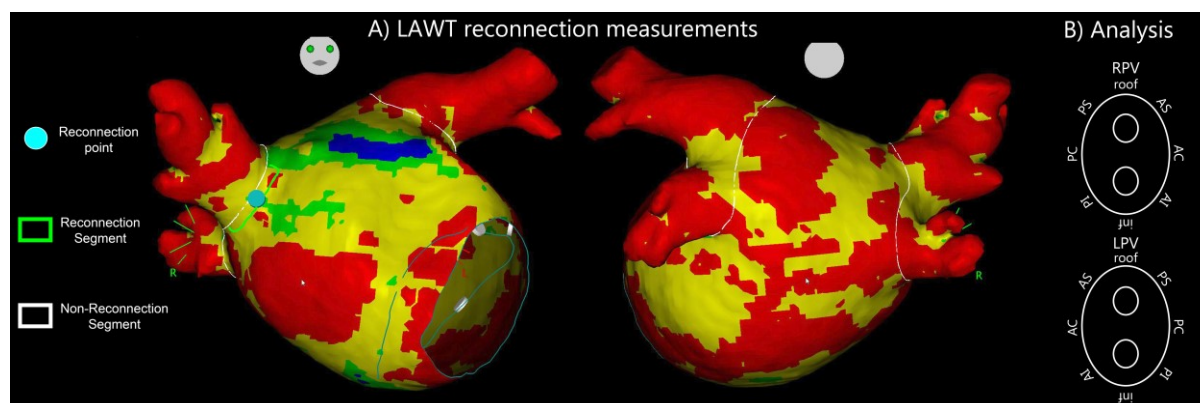


Figure 4. Wall thickness definitions and reconnection site analysis. (A) WT was calculated for the whole circumferential PV line; for each segment individually; and for the reconnection point. **(B)** 16-segment model (AS: Anterosuperior; AC: Anterior carina; AI: Anteroinferior; Inf: Inferior; PI: Posteroinferior; PC: Posterior carina; PS: Posterosuperior; PV: pulmonary vein; WT: wall thickness).

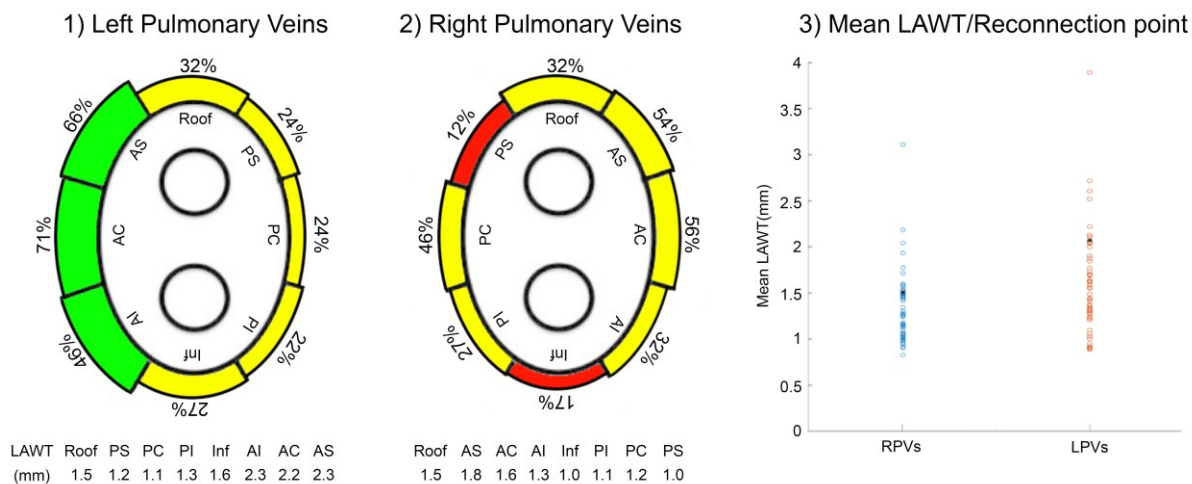


Figure 5. Wall thickness results at AF-redo procedure. The image depicts mean wall thickness of each PV segment and the reconnection rate of each segment (left). The mean wall thickness of the reconnected point was at the 82nd percentile (black dot) of the total circumferential PV line wall thickness at both sides (right).

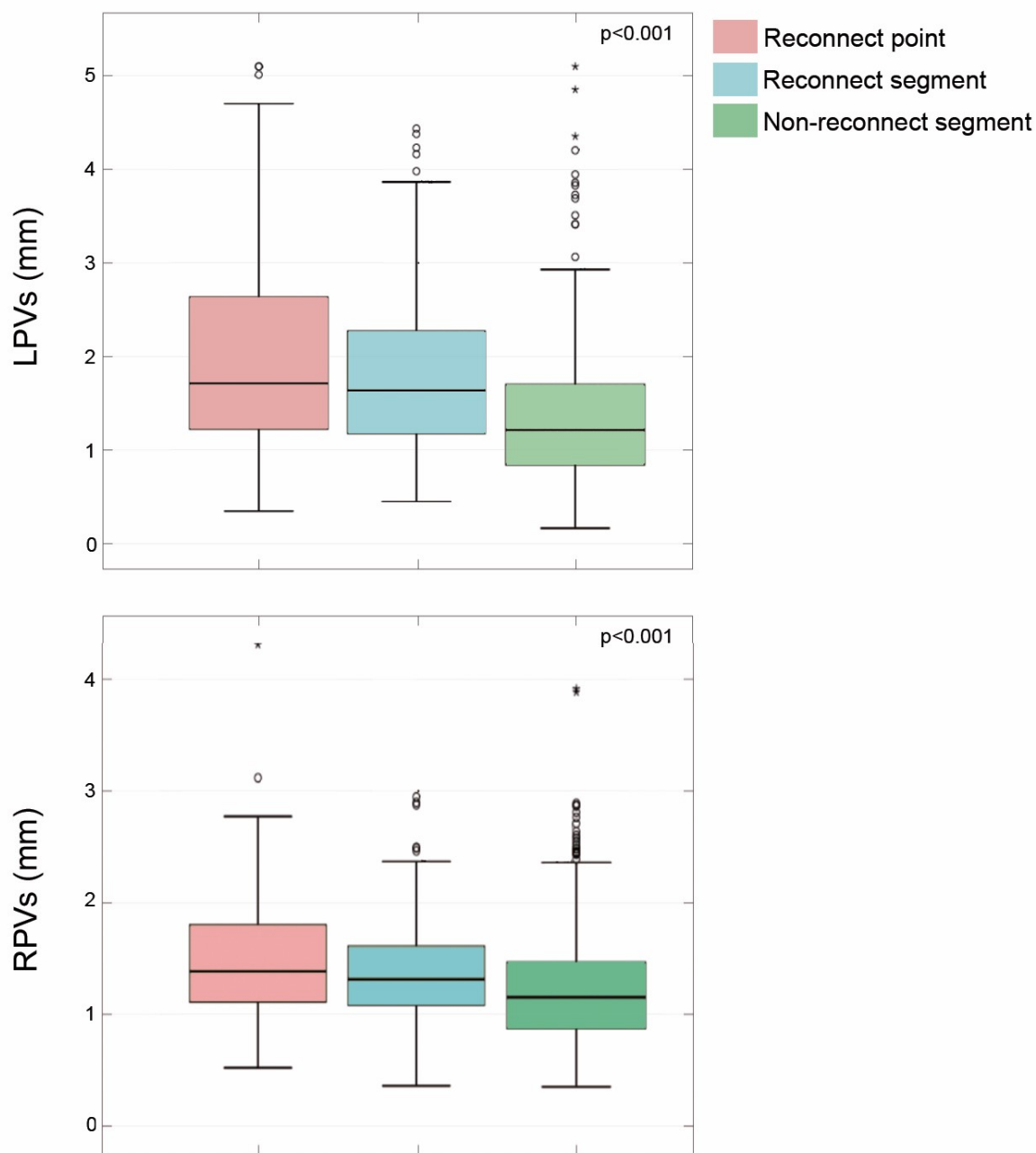


Figure 6. Wall thickness of the reconnected point, the reconnected segment and the rest of the circumferential PV line. P value for comparison between the reconnected point and the rest of the line.

Table 1. Baseline characteristics of the study population

	Total n=60
Age, y	61±10
Male, (%)	43 (72)
Hypertension n (%)	29 (48)
Dyslipemia, n (%)	14 (23,3)
Diabetes, n (%)	9 (15)
LVEF, (%)	58±5,8
LA diameter, mm	41±5,8
BMI, Kg/m2	27.8±8
CHADS-VASc	
0 (%)	12 (20)
1 (%)	7 (11,7)
2 (%)	3 (5)
3 (%)	11 (18,3)
4 (%)	5 (8,3)
≥ 5 (%)	0 (0)
Time since first ablation (months)	Median 19,4 (IQR 9-53)
Type of AF at first ablation n (%)	
• Paroxysmal	38 (63)

<ul style="list-style-type: none"> • Persistent 	12 (37)
Type of Redo n (%) <ul style="list-style-type: none"> • AT/atypical flutter • Paroxysmal • Persistent 	3 (15) 44 (73) 9 (15)

AT: atrial tachycardia; **LA:** left atrium; **LVEF:** left ventricular ejection fraction

Table 2. Protocol for ablation parameters adapted to left atrial wall thickness.

LAWT	Color code	Ablation time (seconds)		RF Energy (Watts)	
		Ant	Post	Ant	Post
< 1mm	Red	12	12	40	35
1-2 mm	Yellow	18	18	40	35
2-3 mm	Green	18	24	50	35
3-4 mm	Blue	30	24	50	35
> 4 mm	Purple	36	30	50	35

LAWT: left atrial wall thickness; **RF:** radiofrequency